Molecular Characterization of Polymer and Polymer Blend Surfaces. Combined Sum Frequency Generation Surface Vibrational Spectroscopy and Scanning Force Microscopy Studies

D. H. GRACIAS,[†,§] Z. CHEN,[†,§]
Y. R. SHEN,[‡,§] AND G. A. SOMORJAI*[,†,§]

Departments of Chemistry and Physics, University of California, Berkeley, California 94720, and Materials Sciences Division, Lawrence Berkeley National Laboratory, Berkeley, California 94720

Received February 1, 1999

Introduction

While molecular surface studies of metal, semiconductor, and oxide surfaces have been the focus of investigations of modern surface science,[1] polymer surfaces have been studied to a much lesser extent. There are many uses of polymer surfaces, such as coatings, adhesives, and lubricants, that would make such studies very desirable. Polymers are also used as implants in the human body (contact lens, joint replacement).[2] Their surface properties determine their biocompatibility, i.e., whether they are accepted or rejected by the other tissues. Exploration of the polymer−protein solution interface on the molecular level could greatly advance our knowledge in the field of biopolymer surface chemistry.[3]

In this Account, we describe our studies of (a) polyolefin (polyethylene, polypropylene) surfaces and (b) polymer blend surfaces (Biospan-S/SP/F blended with phenoxy). The latter are considered for use as implants. We used sum frequency generation (SFG) surface vibrational spectroscopy[4] to monitor the structure at the polymer surface as a function of temperature and blend composition and as the interface is altered from air to water. We also utilized scanning force microscopy[5] (SFM) to monitor the friction and elastic modulus of the same polymer surfaces. In this way, we could correlate surface structure with the surface mechanical properties of the polymers.

Polymers

Figure 1 shows the molecular structure of all the polymers to be discussed in this paper.

Polyethylene and polypropylene were obtained from Aldrich Inc. Commercial films of low-density polyethylene and the phenoxy homopolymer were obtained from Union Carbide. All other polymers were synthesized by Polymer Technology Group, Inc. (Berkeley, CA).

For quantitative SFM measurements of mechanical properties of polyethylene and polypropylene, samples were prepared by melt-casting the polymer pellets on quartz plates and peeling off, and then using the smooth surface in contact with the glass to perform measurements. In all other cases, polymer film samples were prepared by either solvent casting or spin coating and then annealed for several hours to remove the solvent.

IR + Visible SFG Surface Vibrational Spectroscopy

SFG is a second-order nonlinear optical process which can be used to generate a vibrational spectrum of molecules at an interface. The high surface specificity arises from the fact that even-ordered nonlinear processes vanish in centrosymmetric media under the electric-dipole approximation. Hence, the SF signal comes mainly from an interface where centrosymmetry is necessarily broken.

The experimental setup used for our SFG measurement has been described in detail elsewhere.[6] Briefly, it was performed by overlapping a visible and a tunable IR (2500−4000 cm^{-1}) beam on a polymer surface. The surface vibrational spectra were obtained by tuning the IR beam and measuring the SF signal as a function of the IR frequency. Resonant enhancement occurs when the IR frequency scans over surface modes. To determine the orientation of the molecules relative to the surface,[7,8] polarization combinations of ssp (for s-polarized SF

David H. Gracias was born in Bombay in 1972. He completed a five-year integrated M.Sc. in chemistry at IIT, Kharagpur, in 1994. He received his Ph.D. in chemistry with Prof. Somorjai at Berkeley in May 1999. He is currently pursuing postdoctoral research in chemistry at Harvard.

Zhan Chen is a postdoctoral associate in Professor Somorjai's group and a guest scientist in The Polymer Technology Group Inc. He received his B.S. in chemistry from Beijing University and his M.S. in solid-state physics from the Chinese Academy of Sciences. His Ph.D. research, directed by Professor Herbert Strauss at Berkeley, involved Raman spectroscopy, neutron scattering, and IR hole-burning.

Yuen-Ron Shen received his B.S. from the National Taiwan University in 1956 and his Ph.D. from Harvard in 1963. After a year of postdoctoral work at Harvard, he has been a member of the physics faculty at U.C. Berkeley. He has also been associated with the Lawrence Berkeley National Laboratory since 1966. His research interest is in the broad area of interaction of light with matter, with the focus on developing novel linear and nonlinear optical techniques for exploration of new areas of research.

Gabor A. Somorjai received his B.S. in Chemical Engineering from the Technical University, Hungary, in 1956 and his Ph.D. in Chemistry from U.C. Berkeley in 1960. After graduation, he joined the IBM research staff in New York, where he remained until 1964. Since then he has been a member of the faculty in the Department of Chemistry at U.C. Berkeley. He is also a Faculty Senior Scientist in the Materials Sciences Division and Program Leader of the Surface Science and Catalysis Program at the Center for Advanced Materials, Lawrence Berkeley National Laboratory. His research interests lie in the fields of surface chemistry, heterogeneous catalysis, and solid-state chemistry.

* To whom all correspondence should be addressed.
† Department of Chemistry, University of California, Berkeley.
‡ Department of Physics, University of California, Berkeley.
§ Lawrence Berkeley National Laboratory.

10.1021/ar990034f CCC: $18.00
Published on Web 07/08/1999

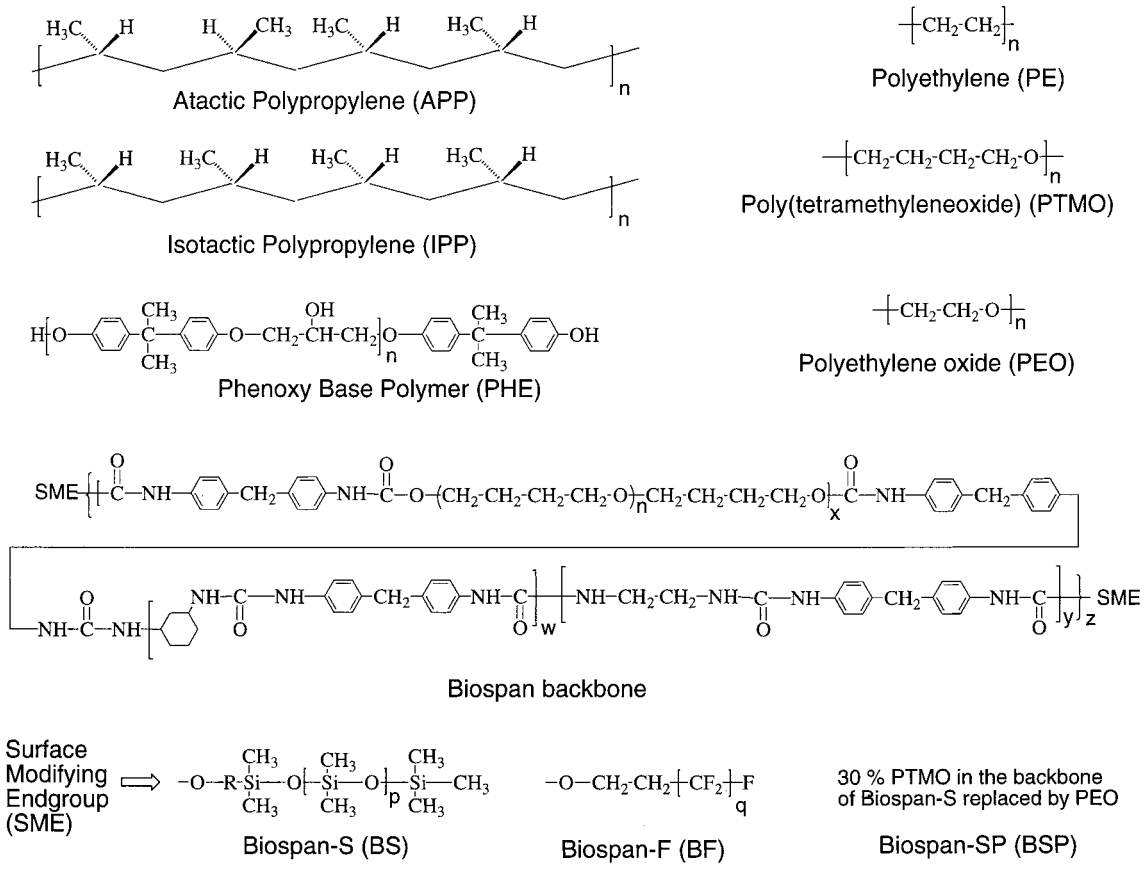

FIGURE 1. Molecular structures of all the polymers reported in this paper.

output, s-polarized visible input, and p-polarized infrared input) and sps were used. Average orientation angles measured are reported with respect to the surface normal.

SFM

SFM involves a sensitive probe interacting with a surface, capable of measuring or applying forces in the range of nanonewtons to micronewtons.

Instruments. We have used three different force microscopes to perform the measurements on the polymer samples, and these are described below.

(a) Quantitative Measurements. To do quantitative measurements of elastic modulus, friction, and hardness on samples of polyethylene and polypropylene, a home-built fiber-optic interferometer type SFM[9] with a tungsten tip was used. This is because the detection scheme used involves interferometry to measure normal (load) and lateral (friction) forces independently and is very accurate and easy to calibrate.

(b) Temperature-Dependent Measurements. To facilitate temperature-dependent measurements, it was necessary to build a walker style SFM[10] which could be evacuated to 10^{-5} Torr, so that we could cool the sample without the temperature of the rest of the instrument being affected. Commercial Si tips (coated with a thin film of tungsten carbide) from NT-MDT were used.

(c) Large-Size Images. To take large-size images (of the order of 200 μm^2) of the polymer blends, we used a commercial Park Scientific M5 SFM.

Measurements with Sharp and Blunt Tips. Our SFM measurements involved mainly two kinds of experiments.

One experiment involved imaging the local structure of the polymer surface and was done with *sharp* tips (*radii of curvature* ~20 nm). The information from such an experiment *complemented* the SFG measurements.

In the other experiments, mechanical measurements of friction force and elastic modulus were carried out at low pressures using *blunt* tips (*radii of curvature* ~1000 nm).[11] The measurements done (applying loads of 1−1500 nN) with blunt tips have higher surface sensitivity (0.1−10 nm) and probe larger contact areas (10^{-4}−10^{-2} μm^2) as compared to those done with sharp tips and thus better facilitate *comparison* with SFG results, which involve averaging over spatial regions of the order of the area of the optical beam (~10^4 μm^2).

Methods Used To Measure Friction, Elastic Modulus, and Hardness.[11] (a) Friction. The frictional force was measured by monitoring the lateral deflection of the cantilever while scanning the cantilever over the same region of the surface, from left to right and then in the opposite direction, i.e., from right to left. The difference between these two scans represents twice the frictional force.

(b) Modulus (Stiffness). The modulus was measured by oscillating the cantilever, with an amplitude of ~1 nm. When the cantilever comes in contact with the sample, the oscillation amplitude is damped. The greater the damping of the oscillation of the cantilever (smaller

amplitude in contact with the surface), the higher is the elastic modulus of the sample, and vice versa.

Another method used to determine the modulus on polypropylene as a function of temperature was to measure interaction force curves between the tip and the surface. In this case, the tip is pushed into *elastic* contact with the surface. The distance moved by the tip into the sample reflects the modulus of the sample.[12]

(c) Hardness. Hardness was measured by *plastic* deformation of the polymer surface. This is done by pushing the tip into the surface with large loads so that a permanent indent is formed on the surface. This indent is then imaged later with the same tip. The hardness is defined as the indentation load divided by the area of the indent.

Measurements on Polyethylene and Polypropylene Surfaces

Surface Structure and Mechanical Properties of Polyethylene and Polypropylene in Air. Polyethylene and polypropylene represent chemically simple polymer systems since they are composed of only carbon and hydrogen. Both polymers have a similar surface energy (~30 dyn/cm[13]) and a glass transition temperature below room temperature (~163 K for polyethylene and ~263 K for polypropylene[14]). Our measurements at room temperature represent measurements on semicrystalline polymers with the amorphous component in the rubbery state.

The polymers studied, in increasing order of percentage crystallinity, were atactic polypropylene (APP) (~2%), low-density polyethylene (LDPE) (20−35%), isotactic polypropylene (IPP) (~63%), high-density polyethylene (~65%), and ultrahigh molecular weight polyethylene (UHMWPE) (70−75%). APP has a lower crystallinity compared to IPP because of a random arrangement of methyl groups on either side of the polymer backbone. The crystallinity of polyethylene is increased by reducing branches on the polymer backbone and by increasing molecular weight.

IR and Raman spectra of LDPE and UHMWPE are identical to published results for polyethylene,[15−17] but their SFG spectra are markedly different, indicating that they have very different surface structures (Figure 2). For LDPE (Figure 2a), the band at 2851 cm^{-1} can be attributed to the CH_2 symmetric stretch and the band at 2926 cm^{-1} to the CH_2 asymmetric stretch. However, for UHMWPE (Figure 2b), the symmetric and antisymmetric CH_2 stretching peaks shift to higher frequencies, which indicates that there are more gauche conformers in the polymer surface.[18,19] The latter is indicative of the crystalline phase of polyethylene, which is composed of thin lamellae, about 10 nm thick, extending up to 10 mm. At the lamellae surface, the molecular chains (which may be as long as 1−10 mm) must fold back on themselves repeatedly. The folding surface then contains a high density of gauche conformers. The average orientation of the methylene group is found to be ~42°. In the case of LDPE, peaks at 2851 and 2926 cm^{-1} indicate that mostly trans conformers exist at the polymer surface, with an average orientation

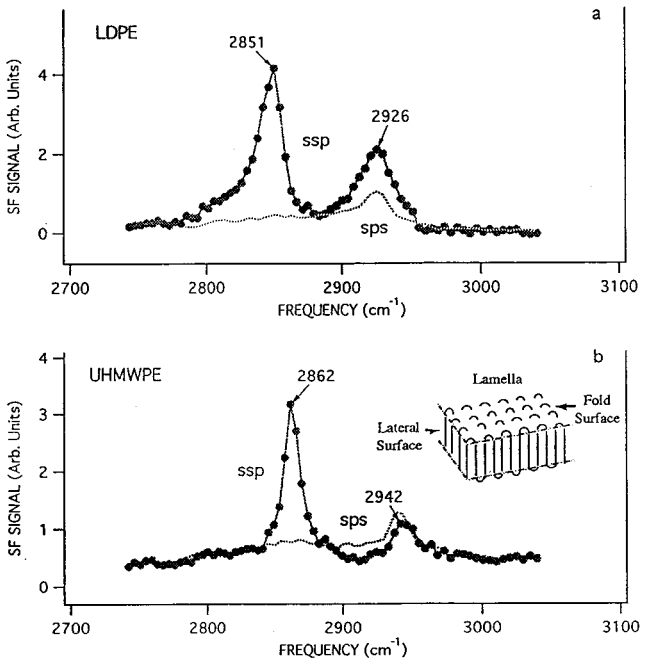

FIGURE 2. SFG spectra of (a) LDPE and (b) UHMWPE.

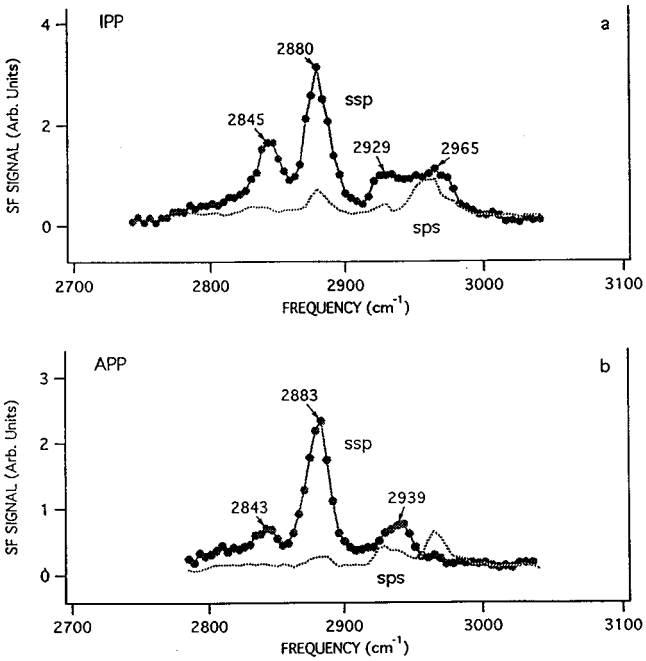

FIGURE 3. SFG spectra of (a) IPP and (b) APP.

of 55° for the CH_2 groups. The random packing of the polymer chains and the disorder of the polymer surface are evidenced by the larger bandwidths of the peaks in the SFG spectrum.

Although the IR and Raman spectra of IPP and APP are very similar, their SFG spectra (Figure 3) are quite different. From the SFG spectra of APP (Figure 3b), the average orientation of the methyl groups at the APP surface was found to be ~30°, while that of the methylene groups is ~59°. This suggests that the hydrocarbon backbone (methylene groups) tends to lie parallel to the surface (to optimize its interaction with the underlying chains), while the methyl groups project out toward the

Table 1. Average Values of the Extrapolated Elastic Modulus E_0 (at Zero Contact Pressure) and Hardness Values (±25%) Measured on the Polymers

polymer	E_0 (GPa)	hardness (MPa)
LDPE	0.47	22
HDPE	1.6	60
IPP	1.09	125
APP	0.15	1.4

surface normal (in order to lower the interfacial energy). Unlike APP, for IPP (Figure 3a), although the methylene group orientation stays the same, ~58°, the average orientation of the methyl groups was found to be ~55°. These results are indicative of the well-documented[20] helical crystalline structure for bulk IPP. Our orientation results can be understood by placing the helical polymer chain more or less lying flat on the surface.

SFM measurements were done on the same polymer surfaces with blunt tips. The modulus and hardness (Table 1) of the less crystalline LDPE and APP are lower than those of the more crystalline HDPE and IPP surfaces. This is consistent with the SFG results that showed enhanced surface ordering for more crystalline IPP and UHMWPE. This implies that increased crystallinity of the bulk polymer results in increased packing or ordering at the surface, which is responsible for a higher modulus and hardness.

Surface Segregation of Bulk Additives and Their Effect on the Surface Structure and Surface Mechanical Properties. We have studied and compared the surfaces of pure LDPE and Commercial LDPE (CLDPE) by SFG and SFM.[21] The difference in these two polymers is the presence of additives in the commercial sample that aid processing and increase stability of the polymers to oxidation.

Whereas the Raman spectra of the two polymers are identical, the SFG spectrum for CLDPE is totally different from that of LDPE (Figure 4). The spectrum exhibits peaks that can be assigned to methoxy-like species,[22,23] which are known to be present in additives. The results indicate that, although the bulk polymers are identical, the surfaces are different, with the additives preferentially segregated to the polymer surface. To see how the surface composition affects the mechanical properties, we have measured the friction and stiffness of the two polymer surfaces as a function of load with SFM using blunt tips (Figure 5). The friction and stiffness measured on the two samples are very different at low loads or small penetration depths. The lower friction of the commercial sample implies that additives segregated to the surface help to lubricate the polymer surface. The lower elastic modulus, on the other hand, means that the additive layer is elastically weaker than the pure LDPE surface layer. We have measured the SFM tip radius and used Hertzian contact mechanics[24] to estimate the penetration depth at which the additives no longer influence the mechanical properties and found it to be 7−8 nm. This is consistent with the fact that the additive layers are seen with SFG and not with Raman spectroscopy. The result also gives an upper limit in the estimate of the surface sensitivity of SFG on polymers.

Changes of the Surface Structure at the Glass Transition of Polypropylene Surfaces. The glass transition in

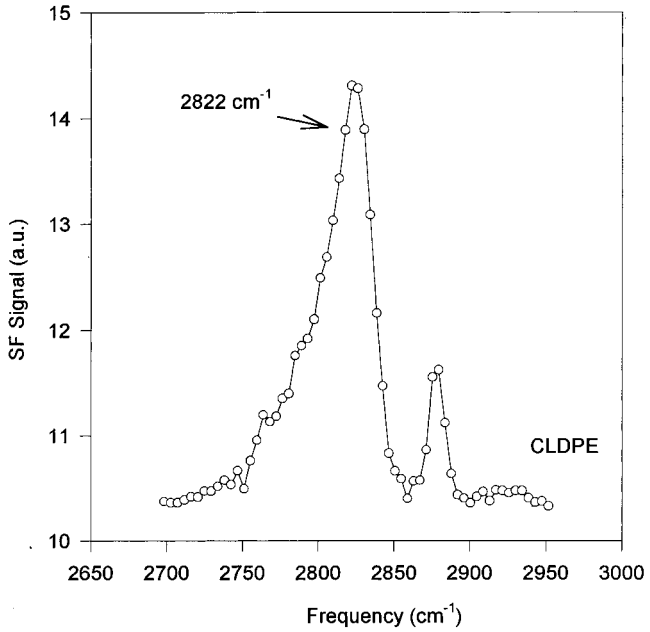

FIGURE 4. SFG spectra of CLDPE.

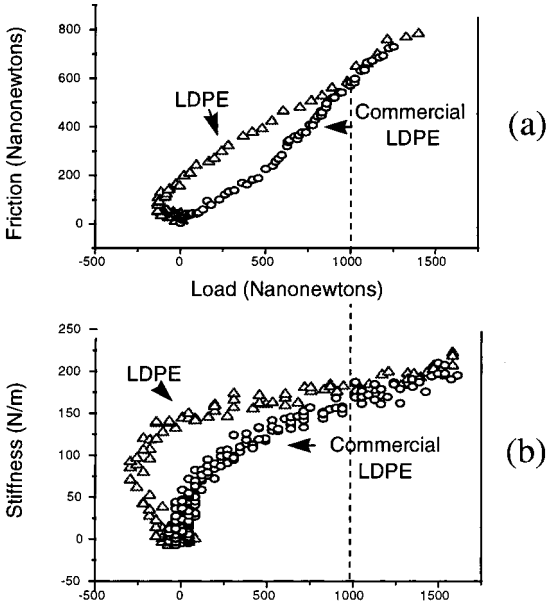

FIGURE 5. Depth profile of (a) friction and (b) stiffness of LDPE and CLDPE.

bulk polymers has been extensively studied.[25] The amorphous component of the polymer undergoes a transition from a rubbery state above the transition temperature to a glassy state below it.

SFG was used to probe the glass transition of the surface of APP and IPP by taking spectra as a function of temperature while cooling the polymer in a vacuum of 10^{-5} Torr. Figure 6 shows the SFG spectra of APP and IPP above and below the glass transition. An increase in the ratio of the symmetric stretch of the CH_2 group to that of the CH_3 group in both APP and IPP was observed on cooling through the glass transition. The observed spectral change across T_g indicates that the CH_2 groups (backbone) become ordered and more polar-oriented at the surface below T_g. Above T_g, the chains are more disordered and

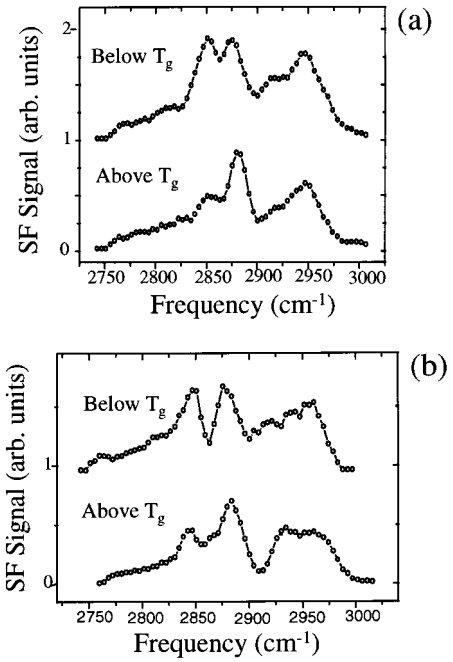

FIGURE 6. SFG spectra of (a) APP and (b) IPP below and above the glass transition temperature.

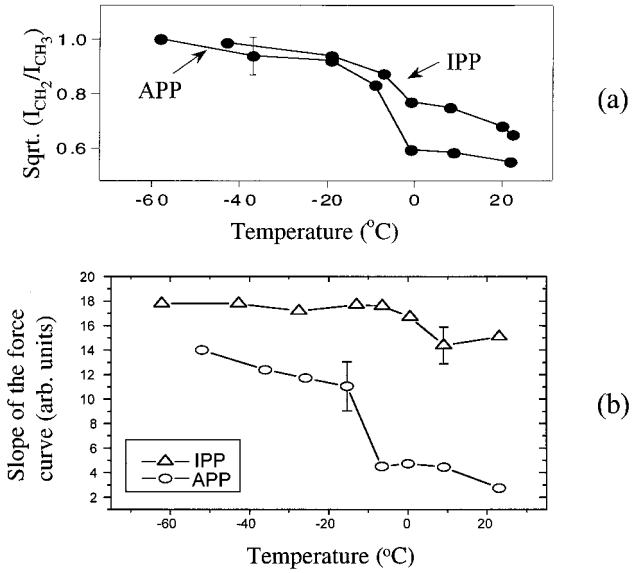

FIGURE 7. (a) SFG peak intensity ratio and (b) the initial slope of the interaction force curve (representing the modulus) as a function of decreasing temperature.

the CH_2 groups more randomly oriented, leading to a reduced CH_2 peak intensity. At all temperatures, the CH_3 groups, being more hydrophobic, orient preferentially away from the surface.

The ratios of the strengths of the individual modes are plotted in Figure 7a to qualitatively describe how the surface structure changes with temperature. The data show that the ratio has a sharp increase in the temperature range between 0 and −20 °C, more prominent for APP than for IPP. Since the bulk glass transition of polypropylene is known to occur in this temperature region, the observed spectral change can be directly correlated to this transition.

Interaction force curves were measured, with blunt tips, on the same surfaces as a function of temperature under a vacuum pressure of 10^{-5} Torr. We monitored the slope of the approach curve and used it as a measure of modulus changes with temperature. For the same tip radius, the higher the slope of the curve, the greater is the elastic modulus.[12] From several temperature runs, the representative changes (∼50 measurements at each temperature) observed for IPP and APP are plotted in Figure 7b. For both IPP and APP, there is an increase in the surface elastic modulus at lower temperatures. For APP, a more rapid change of the modulus occurs between 0 and −20 °C. For IPP, the change is much smaller and occurs around 0 °C.

From bulk studies, it is known that the modulus of the polymer increases by several orders of magnitude in transition to the glass phase. This is because the elastically weak, amorphous polymer above the glass transition transforms into an elastically strong, rigid glass below the glass transition. Thus, it is reasonable to conclude that the changes observed on the surface in this temperature region are also associated with the glass transition.

The temperature dependencies of SFG and SFM results on APP and IPP (Figure 7) show that the enhanced ordering of the backbone (polymer chains) correlates qualitatively with the increased surface modulus.[26] Both are induced by the transition to the glass phase. Since the glass transition involves only the amorphous component of the polymer, we observe a more prominent change in both SFG and SFM measurements for APP (>95% amorphous) as compared to those for IPP (<40% amorphous).

Surface Structure and Composition of Miscible Polymer Blends

Polymer blends provide a way of enhancing the properties of a pure polymer by mixing it with one or more other polymers.[27] The polymer blends in our study consist of two components which are miscible in the bulk. In each case, one component is a phenoxy base polymer (PHE), while the other component is a surface-active polymer containing polyurethane with polytetramethyleneoxide (PTMO) (or partially replacing PTMO with polyethylene oxide (PEO)) soft segments (Biospan) and a surface-modifying end (SME) group composed of either poly(dimethylsiloxane) (PDMS) or fluoroalkyl ($-(-CF_2-)_n-$). The phenoxy polymer in the mixture helps to increase the glass transition of the pure polyurethane component. It can be used to make blends with a T_g between room and body temperatures. Such a glass transition temperature is critical since it means that the blend polymer (which is used as artificial intravenous catheter tubings) will soften after insertion into the vein and return to a round cross section if kinked during insertion. The SME groups are added to the polyurethane component to modify the surface properties of the blend, critical for biocompatibility of the blend. To study the effectiveness of the surface-active polymer in modifying the surface properties, three

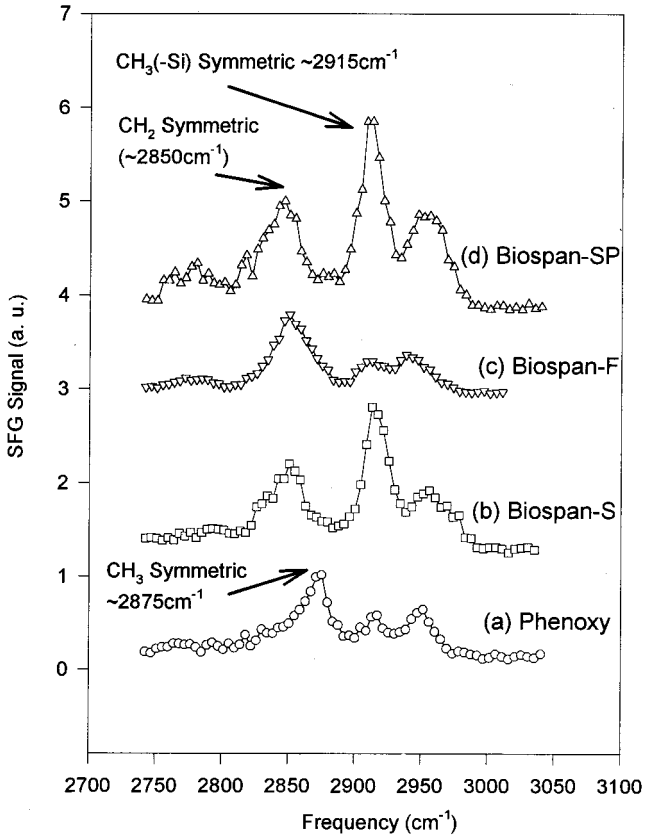

FIGURE 8. SFG spectra of (a) pure PHE, (b) pure BS, (c) pure BF, and (d) pure BSP.

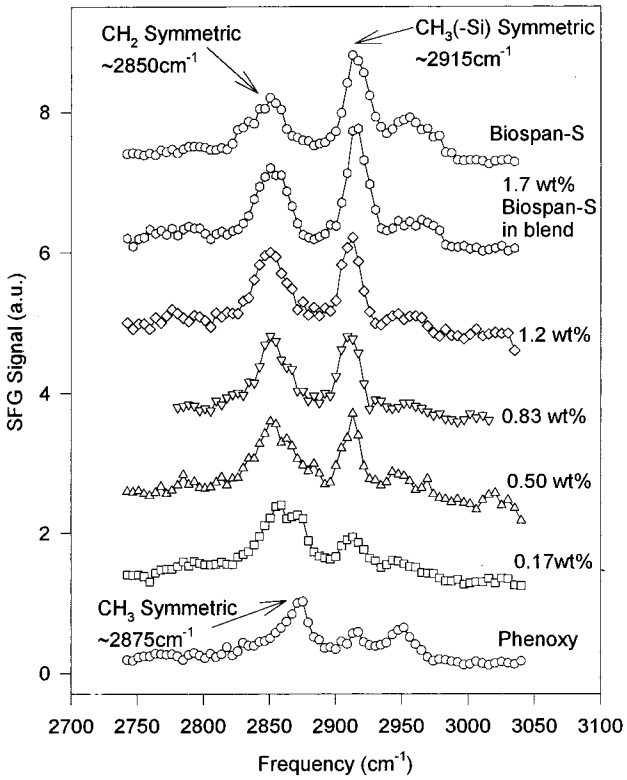

FIGURE 9. SFG spectra of the BS/PHE blend as a function of bulk BS concentration.

polymer blends, Biospan-S (BS)/PHE, Biospan-SP (BSP)/PHE, and Biospan-F (BF)/PHE, were studied.[28,29] BS is a polyurethane with PDMS as end groups. BF has the same polyurethane as BS but is capped by fluoroalkyl end groups. BSP is different from BS in that 30% PTMO in the BS backbone is replaced by PEO. The surface tension of pure PHE, BS, BF, and BSP is 45, 22, 16, and 26 dyn/cm, respectively. The different surface behaviors of the polymers are driven by their different compositions and surface tensions, as will be shown later.

SFG Measurements of Pure Components. The SFG spectrum of pure PHE (Figure 8a) consists of three peaks: the CH_3 symmetric stretch at 2875 cm^{-1}, the CH_2 antisymmetric stretch at 2915 cm^{-1}, and the combined CH_3 antisymmetric stretch and Fermi resonance of CH_2 at 2950 cm^{-1}. The CH_3 symmetric stretch at 2875 cm^{-1} can be taken as the characteristic band for PHE.

For pure BS, the SFG spectrum (Figure 8b) has three prominent peaks: the CH_3 symmetric stretch of PDMS at ~2915 cm^{-1}, the CH_3 antisymmetric stretch and the CH_2 Fermi resonance of PDMS at ~2950 cm^{-1}, and the CH_2 symmetric stretch of Biospan at ~2850 cm^{-1}. This implies a high concentration of PDMS at the surface of the polymer due to its lower surface energy relative to the Biospan backbone of the polymer.

For pure BF (Figure 8c), the characteristic C−F stretching frequency of the SME is out of the range of the current SFG system. The vibrational peak at 2850 cm^{-1} (symmetric CH_2) from the polyurethane part of the polymer can be used as the signature of BF.

The spectrum of BSP (Figure 8d) is very similar to that of BS.

SFG and Contact Angle Measurements of Polymer Blends in Air. (a) BS/PHE. The SFG spectra of the blend surfaces of BS with PHE depend on the bulk concentration of PHE (Figure 9). They show that, as the concentration of BS in the blend increases, BS segregates more to the surface. For a blend with 0.17 wt % BS bulk concentration, the SFG spectrum is very similar to that of pure PHE. The weak 2915-cm^{-1} peak indicates that the surface is not appreciably covered by the PDMS end groups of BS. With increasing BS bulk concentration, the key spectral changes are the weakening of the prominent methyl resonance of PHE at 2875 cm^{-1} and the strengthening of the prominent 2915-cm^{-1} peak of BS. This signifies an enrichment of the BS component at the BS/PHE polymer blend surface. Similarity of the spectra for 1.7 wt % BS/PHE and pure BS indicates that the blend surface is totally covered by BS when its bulk concentration is only 1.7 wt %. Variation of surface tension of the polymer blends correlates well with the relative BS/PHE surface compositions measured by SFG (Figure 10). These results support the claim that the low-surface-energy component (BS) appears to enrich the polymer blend surface as expected.

(b) BF/PHE. Figure 11 shows that the peak at ~2850 cm^{-1} increases as the bulk BF concentration in the BF/PHE blend increases, while the ~2875-cm^{-1} PHE peak decreases. This is indicative of surface enrichment of BF. BF can be detected on the surface with a bulk concentration as low as 0.125 wt %. At 1 wt %, BF completely covers the polymer blend surface. Contact angle measurements

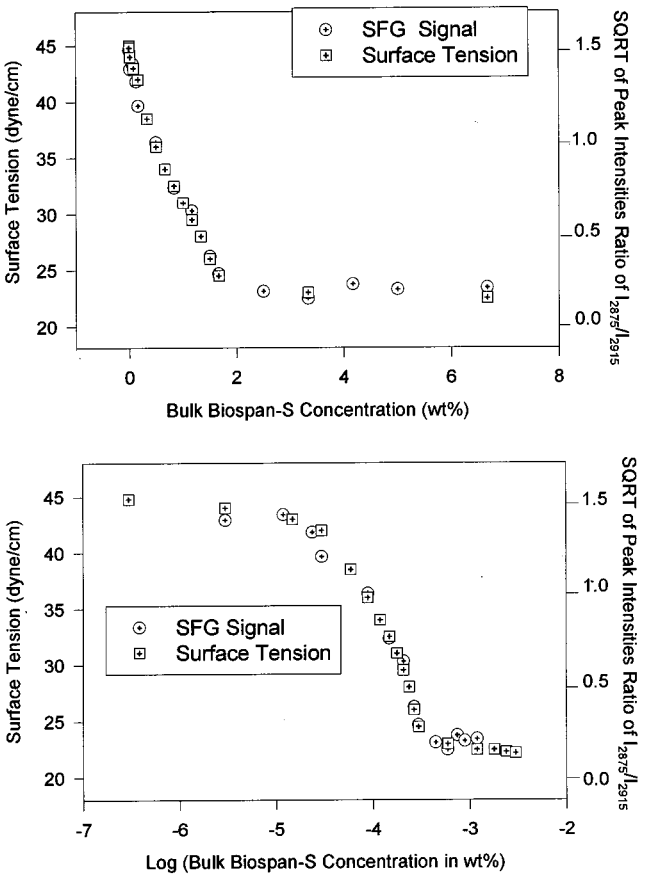

FIGURE 10. SFG peak intensity and surface tension as a function of BS bulk concentration.

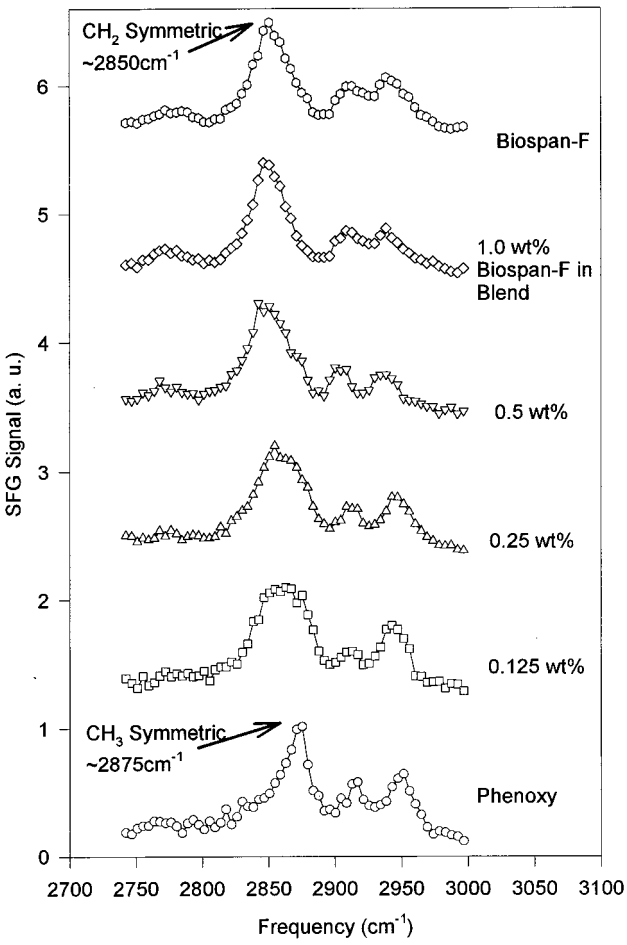

FIGURE 11. SFG spectra of the BF/PHE blends at different BF bulk concentrations.

provide further evidence that BF segregates to the surface and correlate very well with the SFG measurements.

(c) BSP/PHE. Figure 12 shows the SFG spectra of BSP/PHE blends as a function of BSP bulk concentration in wt %. As the concentration of BSP increases in the BSP/PHE blends, the spectra show segregation of BSP to the polymer surface in a fashion very similar to that observed in the other blends. The blend surface is covered by BSP when its bulk concentration reaches 3.5 wt %. The contact angle measurements are consistent with the SFG results.

(d) Comparison. The surface tensions of all three polymer blends are present in Figure 13a. The curves show that the lower the surface energy of the surface-active polymer (surface tension: BF < BS < BSP), the easier it is for it to cover the polymer blend surface (minimum bulk concentration for surface saturation: BF (1 wt %) < BS (1.7 wt %) < BSP (3.5 wt %)). Figure 13b describes a roughly linear correlation between these minimum bulk concentrations and the surface free energy differences between the PHE base polymer and the three surface-active polymer components, BF, BS, and BSP. This relation may be used to predict the wt % of other surface-active polymers that may be added to PHE to fully cover the surface of the polymer blend.

SFG Measurements of Polymer Blend Surfaces in Contact with Water. It is very important to study biopolymer surfaces in the hydrated state because the biopolymers are used as implants in the body, in contact with living tissues or blood. We have studied the surface changes of three polymer blends after they were immersed in water. The three polymer blends are BSP/PHE with 3.5 wt % BSP bulk concentration and BF/PHE with 1 and 5 wt % bulk BF concentration.

When a 3.5 wt % BSP/PHE blend polymer is in contact with water for 1 week, the SFG spectra acquired immediately after the sample is taken out of water (Figure 14) show that the surface is still dominated by BSP. However, the surface concentration of the BSP end groups (PDMS) decreases, so that the surface is now covered more by the polyurethane part of the BSP. The changes are similar to that seen in pure BS after it has been in contact with water.[30] Even though PHE is more hydrophilic than BSP, our results indicate that the interaction of water with the polymer is unable to overcome the diffusion barrier for PHE to emerge. The interaction is, however, strong enough to drive rearrangement of the backbone and end groups in BSP (and BS), such that the more hydrophobic PDMS tends to submerge and the more hydrophilic polyurethane backbone tends to emerge.

PHE was not detected on the 1 wt % BF/PHE surface in air. However, after PHE was in contact with water for 5 days, the characteristic peak at ~2875 cm^{-1} showed up (Figure 15a). This indicates that the PHE component has

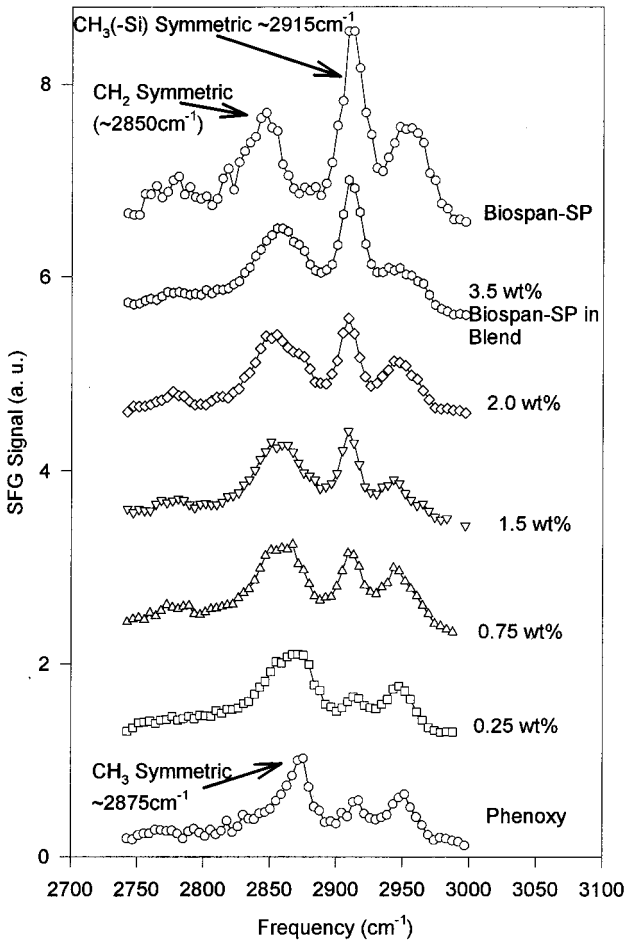

FIGURE 12. SFG spectra of BSP/PHE blends at different BSP bulk concentrations.

emerged to the surface due to the more hydrophilic nature of PHE than BF. After this BF/PHE polymer blend was dried in the air, the PHE component resubmerged, although only partially, as the ~2875-cm^{-1} peak can still be detected by SFG. Figure 15b shows that, for 5 wt % BF/PHE blend, the surface is always completely dominated by BF, whether it is in air or in water. The PHE component is barely visible in the SFG spectra, even after the surface is immersed in water for 1 week.

SFM Measurements of Polymer Blends. In SFM measurements of polymer blends, we used sharp tips to probe the local structure of the polymer surface. For BS concentrations lower than 0.17 wt % (Figure 16c), the surface appears featureless and resembles that of pure PHE (Figure 16a). This correlates well with the SFG result, which indicated that the blend surface consists mainly of PHE in this concentration regime. Figure 16d is an image obtained at concentrations higher than 1.7 wt %. The picture shows many holes similar to that observed on the surface of pure BS (Figure 16b), suggesting that the surface is covered by BS, as was observed by SFG.

For BS bulk concentrations in the range of 0.17−1.7 wt %, when the SFG and contact angle data show a transition from a PHE-covered surface to a BS-covered surface, topographic SFM images (Figure 17a) exhibit a domain structure, very similar to the patterns observed

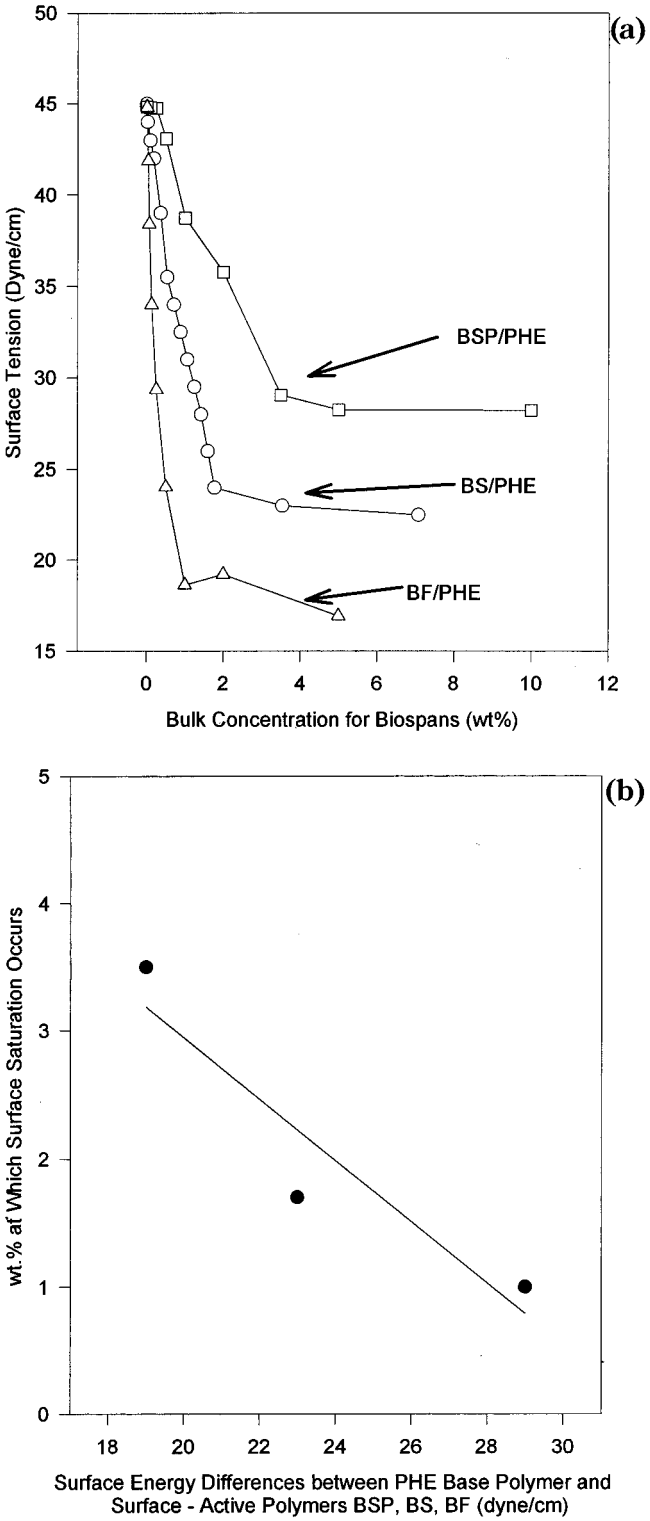

FIGURE 13. (a) Comparison of surface tensions of three polymer blends: BS/PHE, BSP/PHE, and BF/PHE. (b) Linear correlation between the wt % at which saturation of the surface-active component occurs and the surface free energy differences of the PHE base polymer and the surface-active polymers BF, BS, and BSP.

in other phase-segregated macromolecular systems.[31] The average height of the ridges is around 4 nm, which is the height of stacking of a few molecules. It is interesting to know the composition of the ridges and the base in this

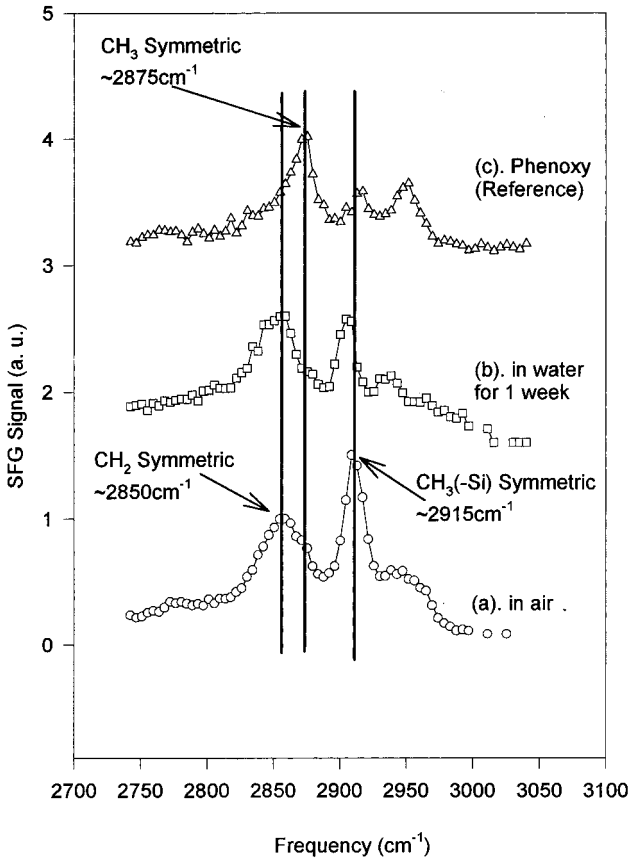

FIGURE 14. SFG spectra of BSP/PHE with 3.5 wt % BSP bulk concentration in air and after in contact with water.

image. This we achieved by measuring the surface friction of the pure components and the blend surface independently with the SFM using the same sharp tip. The friction of the pure PHE surface was found to be higher than that of BS. This can be explained by the higher surface energy of PHE as compared to that of BS, which results in a larger contact area between the SFM tip and the surface and hence increases the friction. The friction image of the blend is shown in Figure 17c. It was found that the ridges have a higher friction than the base, which indicates a PHE-rich region.

Complementarity of SFG and SFM Measurements. The adsorption of the lower surface energy component at the polymer blend surface (Figure 10) is very similar to what has been universally observed for binary liquid mixtures of small organic molecules. However, we observe that the changes of the surface tension (γ) as a function of the concentration of the component of lower surface energy (C) are different for polymer blends and liquid mixtures. The usual analysis of such a function of a binary liquid mixture uses the Gibbs equation.[32] In a typical $\gamma-\log C$ plot for a liquid mixture, the slope of the curve remains essentially unchanged in a given region where the surface tension keeps changing, indicating that the surface concentration of the surface-active component reaches a constant maximum value at the liquid surface. In our study shown in Figure 10, both the surface composition and the surface tension change simultaneously with the BS bulk concentration in the region

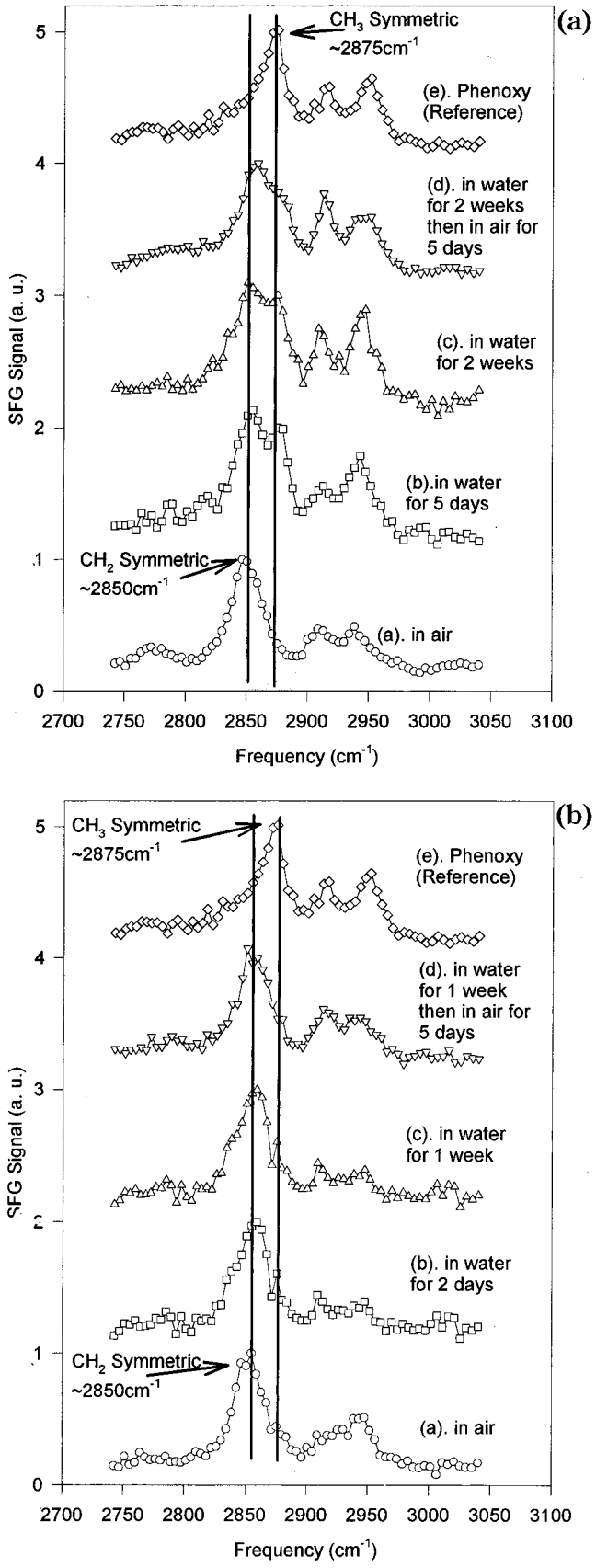

FIGURE 15. (a) SFG spectra of BF/PHE with 1 wt % BF bulk concentration in air, after being in contact with water, and later, dried in air again. (b) SFG spectra of BF/PHE with 5 wt % BF bulk concentration in air, after being in contact with water, and later, dried in air again.

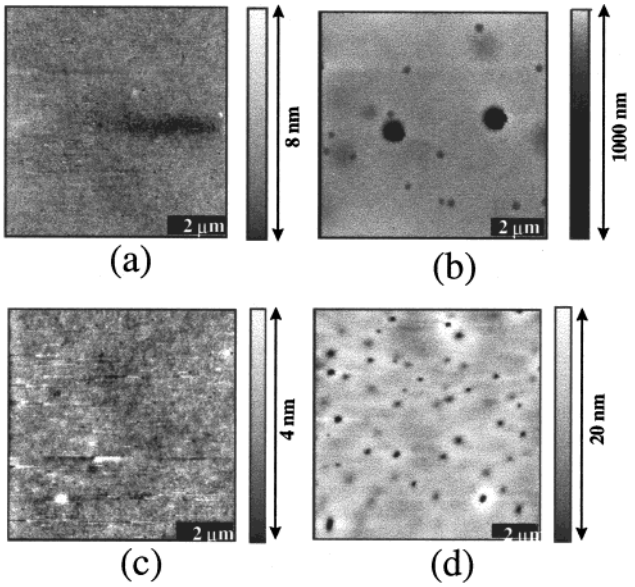

FIGURE 16. SFM images of pure PHE and pure BS and the blends at low and high BS concentrations.

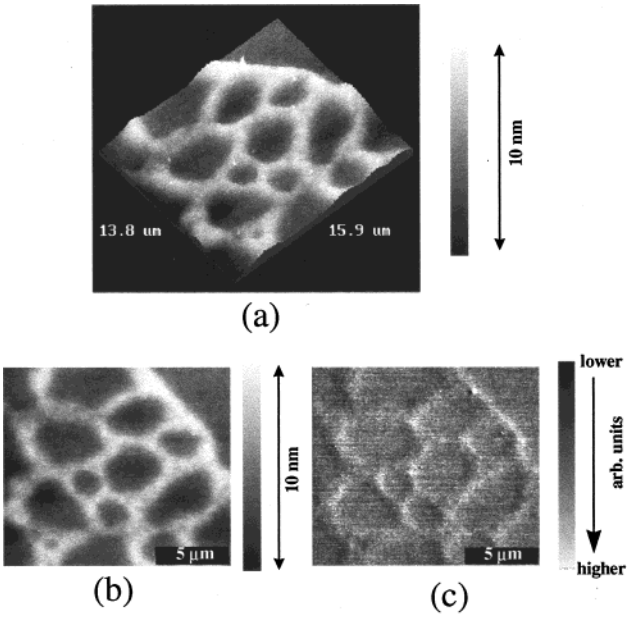

FIGURE 17. SFM images of the blend at intermediate blend concentrations showing surface segregation of the blends. (a,b) Topography; (c) friction.

below 1.7 wt %. Then, both reach a constant value when the BS bulk concentration is 1.7 wt %. The different behaviors between the polymer blend and the liquid mixture are probably due to segregation of polymer components on the surface, as revealed by SFM, which does not occur in liquid mixtures. This is an example which shows that SFM can be used to complement SFG measurements to yield a more complete picture of the polymer surface structure for different bulk compositions of the polymer blend.

Conclusion

SFG and SFM are monolayer-sensitive techniques that permit determination of structure and composition as well as mechanical properties of friction and elastic modulus of the same polymer surface. Correlation of surface structure with surface mechanical properties permits the understanding of how molecular orientation and arrangement at the surface control the friction and elastic modulus of the surface. This combination of SFG and SFM techniques has been utilized to study polyethylene and polypropylenes of different molecular weights (LDPE, HDPE, and UHMWPE) and structures (APP and IPP). The surface structures of these polymers were determined along with the variation of surface structure above and below the glass transition temperature. The monolayer surface sensitivities of both SFG and SFM techniques were demonstrated when surface segregation of bulk additives used to control surface properties was actually detected.

Polymer blends that are being developed for body implant application greatly benefit from the combined use of SFG and SFM. The variation of surface structure and composition with changes of bulk composition of the blends could be monitored in air and in water. Segregation of the polymer with the hydrophobic end groups to the surface was detected in air, while segregation of the more hydrophilic polymer constituent to the surface was detected at the polymer−water interface. Deviation from the ideal case of surface/bulk segregation predicted by the Gibbs equation for liquid mixtures was observed as the bulk composition of the blend was altered.

This work was supported by the Director, Office of Energy Research, Office of Basic Energy Sciences, and the Materials Sciences Division of the U.S. Department of Energy under Contract No. DE-AC0376SF00098. We acknowledge additional support from Polymer Technology Inc.

References

(1) Somorjai, G. A. *Introduction to Surface Chemistry and Catalysis*; Wiley: New York, 1994.
(2) Recum, A. F. *Handbook of Biomaterials Evaluation: Scientific, Technical, and Clinical Testing of Implant Materials*; Macmillan Publishing Co.: New York, 1986.
(3) Cooper, S. L.; Peppas, N. A. *Biomaterials: Interfacial Phenomena and Applications*; ACS Advances in Chemistry Series 199; American Chemical Society: Washington, DC, 1982.
(4) Shen, Y. R. Surface properties probed by second-harmonic and sum-frequency generation. *Nature* **1989**, *337*, 519−525.
(5) Binnig, G.; Quate, C. F.; Gerber, Ch. Atomic force microscope. *Phys. Rev. Lett.* **1986**, *56*, 930−933.
(6) Zhu, X. D,; Suhr, H.; Shen, Y. R. Surface vibrational spectroscopy by infrared-visible sum frequency generation. *Phys. Rev. B* **1987**, *35*, 3047−3050.
(7) Guyot-Sionnest, P.; Hunt, J. H.; Shen Y. R. Sum-frequency vibrational spectroscopy of a Langmuir film: study of molecular orientation of a two-dimensional system. *Phys. Rev. Lett.* **1987**, *59*, 1597−1600.
(8) Hirose, C.; Akamatsu, N.; Domen, K. Formulas for the analysis of surface sum-frequency generation spectrum by CH stretching modes of methyl and methylene groups. *J. Chem. Phys.* **1992**, *96*, 997−1004.

(9) Rugar, D.; Mamin, H. J.; Guethner, P. Improved fiber-optic interferometer for atomic force microscopy. *Appl. Phys. Lett.* **1989**, *55* (25), 2588−2590.
(10) Frohn, J.; Wold, J. F.; Besocke, K.; Teske, M. Coarse tip distance adjustment and positioner for a scanning tunneling microscope. *Rev. Sci. Instrum.* **1989**, *60*, 1200−1201.
(11) Gracias, D. H.; Somorjai, G. A. Continuum force microscopy study of the elastic modulus, hardness and friction of polyethylene and polypropylene surfaces. *Macromolecules* **1998**, *31*, 1269−1276.
(12) Burnham, N. A.; Colton, R. J.; Pollock, H. M. Interpretation of force curves in force microscopy. *Nanotechnology* **1993**, *4*, 64−80.
(13) Wu, S. *Polymer Interface and Adhesion*; Marcel Dekker: New York, 1982.
(14) Baer, E. Advanced polymers. *Sci. Am.* **1986**, *255*, 156−165.
(15) Hummel, D. O. *Polymer Spectroscopy*; Verlag Chemie: London, 1973.
(16) Bentley, P. A.; Hendra, P. J. Polarised FT Raman studies of an ultrahigh modulus polyethylene rod. *Spectrochim. Acta Part A* **1995**, *51*, 2125−2131.
(17) Zhang, D.; Shen, YR.; Somorjai, GA. Studies of surface structures and compositions of polyethylene and polypropylene by IR plus visible sum frequency vibrational spectroscopy. *Chem. Phys. Lett.* **1997**, *281*, 394−400.
(18) Snyder, R. G.; Strauss, H. L.; Elliger, C. A. C−H stretching modes and the structure of *n*-alkyl chains. I. Long, disordered chains. *J. Phys. Chem.* **1982**, *86*, 5145−5150.
(19) Hostetler, M. J.; Stokes, J. J.; Murray, R. W. Infrared spectroscopy of three-dimensional self-assembled monolayers—*n*-alkanethiolate monolayers on gold cluster compounds. *Langmuir* **1996**, *12*, 3604−3612.
(20) Cowie, J. M. G. *Polymers: Chemistry and Physics of Modern Materials*; Intext Eduational Publishers: New York, 1981.
(21) Gracias, D. H.; Zhang, D.; Shen. Y. R.; Somorjai. G. A. Surface chemistry property relationship of low-density polyethylene: an IR+visible sum frequency generation spectroscopy and atomic force microscopy study. *Tribol. Lett.* **1998**, *4* (3−4), 231−235.
(22) Miragliotta, J.; Polizzotti, R. S.; Rabinowitz, P.; Cameron, S. D.; Hall, R. B. IR-visible sum-frequency generation study of methanol adsorption and reaction on Ni(100). *Chem. Phys.* **1990**, *143*, 123−130.
(23) Colthup, N. B.; Daly, L. H *Introduction to Infrared and Raman Spectroscopy*; Academic Press Inc.: New York, 1994.
(24) Johnson, K. L *Contact Mechanics*, 1st ed.; Cambridge University Press: New York, 1987; pp 84−105.
(25) S. Matsuoka, *Relaxation Phenomena in Polymers*; Carl Hanser Verlag: New York, 1992.
(26) Gracias, D. H.; Zhang, D.; Lianos, L.; Ibach, W.; Shen Y. R.; Somorjai G. A. A study of the glass transition of Polypropylene surfaces by Sum-Frequency Vibrational Spectroscopy and Scanning Force Microscopy. *Chem. Phys.* **1999**, *245*, 275−282.
(27) Han, C. D., Ed. *Polymer blends and composites in multiphase systems*; American Chemical Society: Washington, DC, 1984; p 206.
(28) Zhang, D.; Gracias, D. H.; Ward, R.; Gauckler, M.; Tian, Y.; Shen, Y. R.; Somorjai, G. A. Surface studies of polymer blends by sum frequency vibrational spectroscopy, atomic force microscopy, and contact angle goniometry. *J. Phys. Chem.* **1998**, *102*, 6225−6230.
(29) Chen, Z.; Ward, R.; Tian, Y.; Eppler, A.; Shen, Y. R.; Somorjai, G. A Surface composition of biopolymer blends Biospan-SP/Phenoxy and Biospan-F/Phenoxy observed with SFG, XPS, and contact angle goniometry. *J. Phys. Chem. B* **1999**, *103*, 2935−2942.
(30) Zhang, D.; Ward, R.; Shen, Y. R.; Somorjai, G. A. Environment-induced surface structural changes of a polymer: An in situ IR plus visible sum-frequency spectroscopic study. *J. Phys. Chem.* **1997**, *101*, 9060−9064.
(31) Bar, G.; Thomann, Y.; Brandsch, R.; Cantow, H.-J.; Whangbo, M.-H. *Langmuir* **1997**, *13*, 14, 3807−3812.
(32) Adamson, A. W. *Physical Chemistry of Surfaces*; Wiley-Interscience Publication: New York, 1982.

AR990034F